Detonation capturing for stiff combustion chemistry

EINDHOVEN UNIVERSITY OF TECHNOLOGY
Department of Mathematics and Computing Science

RANA 95–06
April 1995

Detonation Capturing for Stiff Combustion Chemistry

by

A.C. Berkenbosh, E.F. Kaasschieter
J.H.M. ten Thije Boonkkamp, R. Klein

Reports on Applied and Numerical Analysis
Department of Mathematics and Computing Science
Eindhoven University of Technology
P.O. Box 513
5600 MB Eindhoven
The Netherlands
ISSN: 0926–4507

Detonation Capturing for Stiff Combustion Chemistry

A.C. Berkenbosch, E.F. Kaasschieter, J.H.M. ten Thije Boonkkamp
Department of Mathematics and Computing Science,
Eindhoven University of Technology,
P.O. Box 513, 5600 MB Eindhoven, The Netherlands

and

R. Klein
Institut für Technische Mechanik,
RWTH Aachen,
Templergraben 64, 52056 Aachen, Germany.

Abstract

We consider the numerical computation of one-dimensional detonation waves. Detonation waves are travelling wave solutions of the reactive Euler equations. An essential difficulty in the numerical computation of detonation waves is the occurrence of nonphysical solutions. In order to study this problem we consider a 2×2 model problem. For this model problem it is illustrated that nonphysical solutions are weak detonation waves. This is used to obtain a simple criterion which ensures that, also for relatively large mesh sizes, the numerical solution approximates the physically correct weak solution. Finally, we extend this criterion to the reactive Euler equations. Numerical results support the use of this criterion to exclude nonphysical weak detonation waves.

A.M.S. Classifications: 35L60, 35L65, 65M06
Keywords : Conservation laws, reactive Euler equations, detonation waves, ZND model, splitting method.

1 Introduction

In simulations of the flow of a reacting gas mixture, chemical reactions between the constituent gases need to be modelled together with the fluid dynamics. Problems of this form arise, for example, in combustion [5, 10]. The conservation laws for reacting gas flow and the theory of chemical kinetics form the basis of combustion theory. These equations represent the conservation of mass, momentum and energy of the total mixture and the change of composition of the gas mixture due to reaction.

A considerable simplification of these equations is possible if we restrict ourselves to one-dimensional detonations. Detonation waves are propagating so fast that molecular diffusion, thermal conductivity and viscosity are usually unimportant, and therefore they are ignored. If effects of walls, heat sources and external forces are also ignored, we essentially obtain the Euler equations of gas dynamics, completed with the continuity equations for the various species (see (3.1) below). These latter equations include source terms describing the chemical reactions. The complete system of equations is often referred to as the reactive Euler equations. In many model computations, the chemical reactions are described by the ignition model or the law of mass action and Arrhenius' law [10]. In this paper the ignition model is used. In this model there exists an ignition temperature T_{ign} such that the reaction rate is very large when the temperature is above the ignition temperature and zero otherwise.

In this paper we consider detonation waves described by the ZND model (a model developed by Zel'dovich, von Neumann and Döring) [5, 10]. The ZND model assumes that a detonation wave consists of an ordinary nonreacting shock wave followed by a reaction zone. Hence, due to a strong leading shock front the temperature jumps to a value higher than some ignition temperature and a reaction is started.

The reactive Euler equations are a system of first order hyperbolic conservation laws. Since detonation waves have a discontinuous structure, including a strong leading shock front, we consider weak solutions of hyperbolic differential equations. A difficulty is that weak solutions turn out to be nonunique and we have to characterise the unique "physically relevant" weak solution. In case of the ZND model for detonation waves, this unique weak solution is characterised by Jouguet's rule, which says that the flow in a front attached frame of reference is supersonic in the unburnt gases ahead of the wave and subsonic or sonic in the burnt gases behind the wave. In the former case, one speaks of a strong or overdriven detonation wave, while a wave with sonic outflow is called a Chapman-Jouguet detonation wave [4].

When attempting to solve the reactive Euler equations numerically, we encounter problems that are absent in nonreacting flows. Apart from an increase in the number of equations, the main difficulty is the fact that, in general, the time scales of the chemical reactions are very small compared to the time scale of the fluid dynamics. For fast reactions it is possible to obtain stable numerical solutions that look reasonable and yet are completely wrong, because the discontinuities have the wrong locations. Thus, the numerical reaction waves are propagating at nonphysical wave speeds. This phenomenon has been observed by several other authors [3, 8]. In this paper it is shown that these "wrong solutions" turn out to be approximations of nonphysical weak solutions (i.e. weak detonation waves).

In general the nonphysical weak detonation waves are only observed if the ignition temperature is close to the temperature of the unburnt gas. In this case, due to numerical diffusion, the temperature is raised above the ignition value and the reaction is started artificially. If the reaction is fast enough, then the gas is completely burnt in the next time step and the discontinuity is shifted to a cell boundary. Therefore, it is not surprising that nonphysical wave speeds of one cell per time step can be observed for fast reactions. For these relatively low values of the

ignition temperature, numerical experiments show that only on very fine meshes the numerical solution will approximate the correct weak solution. In most practical cases we cannot afford such fine meshes and therefore, we want a criterion that excludes the nonphysical weak detonation waves also on relatively coarse meshes.

It is important to remark that in practical applications the ignition temperature is much higher than the temperature of the unburnt gas and our numerical results illustrate that for these ignition temperatures, the nonphysical weak solutions will not occur.

We observe the same essential numerical difficulty of approximating incorrect weak solutions for low ignition values in the simplified detonation model studied by Majda in [9]. This model is a 2×2 system of equations which bears the analogous relationship to the reactive Euler equations as Burgers' equation does to the ordinary Euler equations. Also for this model problem the correct solution is obtained here as the ignition temperature increases to more realistic values.

In this paper we present theoretical insights in order to explain the strong influence of the ignition temperature on the numerical solution for the simplified detonation model. The incorrect weak solution appears to be a weak detonation wave followed by an ordinary shock wave, while the physically correct solution is a strong detonation wave propagating with speed $s > 0$. It is shown that nonphysical solutions are excluded, if the temperature in the burnt gas directly behind the detonation wave is larger than the final state of a weak detonation wave propagating with speed s. Subsequently, this is used to obtain a simple criterion, which ensures that also for relatively coarse meshes, the numerical solution approximates the physically correct detonation wave speed. Furthermore, we extend this criterion to the reactive Euler equations.

The criterion simply states that the ignition temperature should exceed a certain threshold value that is determined by the thermodynamical features of the mixture. Our numerical computations illustrate convincingly that the correct detonation speed is obtained, even if the Damköhler number is large enough to enforce the thickness ℓ_r of the associated ZND detonation to occupy merely a tiny fraction of a numerical mesh width Δx.

In fact, we consider cases, where $\ell_r \approx 10^{-5}\Delta x$. Certainly, in this situation any information about the detailed structure of the wave is lost. Moreover, any dynamics or stability behaviour of the detonations is not represented, since that is inherently due to effects of the inner structure of the detonations. However, the major flaw of the generation of nonphysical weak detonations is overcome.

We emphasise that such a choice is in fact more realistic than an ignition temperature that is very close to the unburnt gas temperature; reactive gases typically require considerable heating before the chemical reactions become self-sustained. From a mathematical point of view, this is a consequence of a characteristic exponential (Arrhenius-type) behaviour of the reaction rate laws, which guarantees the rates to be exponentially small even for temperatures relatively close to the burnt gas temperature. On the other hand, from a chemical point of view, this freezing of the chemistry up to considerable temperatures can be due to a chemical kinetic competition for radical species, which for low temperatures is completely on the side of the radical consuming reactions. In fact, recent studies of hydrogen as well as hydrocarbon combustion systems show that there typically exists a kinetically determined temperature threshold of about 1100 K [6].

If highly precompressed gas mixtures are considered with temperatures that are in fact close to this kinetic threshold, one has to take the standard considerations that exclude weak detonations with a heavy grain of salt. Due to processes of sequential auto-ignition, weak detonation fronts can in fact occur and a numerical scheme that automatically suppresses them, suppresses an important piece of the physics. However, to our knowledge, the numerical simulation of combustion processes in this transition regime, with sufficient focus on the problem of physical and

nonphysical detonations structures, is an open problem yet. We do not intend to suggest a solution here.

This paper is organised as follows. In the next section one-dimensional hyperbolic conservation laws with source terms, and their weak solutions are introduced. In Section 3 the reactive Euler equations are presented. The Chapman-Jouguet model and the ZND model are briefly described. A simplified detonation model is presented in Section 4. Furthermore, we describe the analogues of the Chapman-Jouguet model and the ZND model for this 2×2 model problem. In Section 5 we restrict ourselves to the simplified detonation model. We present the well-known first order splitting method, where, for the sake of simplicity, we only describe a combination of Roe's method and the backward Euler method. In this section we show that nonphysical solutions are always weak detonation waves. The latter property is used to obtain the desired criterion that excludes the nonphysical weak solutions. In Section 6 we present some numerical results for the simplified detonation model that illustrate the preceding analysis. Finally, in Section 7 we extend the previously derived criterion to the reactive Euler equations and present some numerical results for the reactive Euler equations that support this criterion.

2 Hyperbolic Conservation Laws with Source Terms

In the following we consider one-dimensional conservation laws with source terms. It is assumed that the source terms are only dependent on the solution $\mathbf{u}$. The general form of such conservation laws is

$$\frac{\mathrm{d}}{\mathrm{d}t}\int_{x_L}^{x_R} \mathbf{u}(x,t)\mathrm{d}x \;=\; \mathbf{f}(\mathbf{u}(x_L,t)) - \mathbf{f}(\mathbf{u}(x_R,t)) + \int_{x_L}^{x_R} \mathbf{q}(\mathbf{u}(x,t))\mathrm{d}x. \tag{2.1}$$

Conservation laws of this form occur, among others, in the theory of reacting gas flow [5, 10]. Assume that the solution $\mathbf{u} : \mathbb{R} \times [0,\infty) \to \mathbb{R}^m$ and the flux function $\mathbf{f} : \mathbb{R}^m \to \mathbb{R}^m$ are continuously differentiable and let the source term $\mathbf{q} : \mathbb{R}^m \to \mathbb{R}^m$ be continuous. Then, since (2.1) should hold for arbitrary x_L and x_R, it is clear that $\mathbf{u}$ satisfies

$$\frac{\partial}{\partial t}\mathbf{u}(x,t) + \frac{\partial}{\partial x}\mathbf{f}(\mathbf{u}(x,t)) \;=\; \mathbf{q}(\mathbf{u}(x,t)). \tag{2.2a}$$

This is the differential form of the conservation law. In order to obtain an initial value problem we add initial data to (2.2a), i.e.

$$\mathbf{u}(x,0) \;=\; \mathbf{u}^0(x), \quad \forall x \in \mathbb{R}. \tag{2.2b}$$

The assumption of the solution of (2.1) to be continuously differentiable is too strong, since in practice discontinuous solutions $\mathbf{u}$ of (2.1) occur [5, 7, 10]. This is the reason why weak solutions of the initial value problem (2.2) are interesting. These weak solutions are obtained from multiplying (2.2a) with an arbitrary test function $\varphi \in C_0^1(\mathbb{R} \times [0,\infty))$ (i.e. φ vanishes for $|x| + t$ large) and, subsequently, partially integrating this equation in space and time. This leads to the following definition.

Definition 2.1 *A bounded measurable function* $\mathbf{u}$ *is called a* weak solution *of the conservation law* (2.2a) *with bounded initial data* (2.2b) *if*

$$\int_0^\infty \int_{-\infty}^\infty \left\{ \mathbf{u}(x,t) \frac{\partial}{\partial t}\varphi(x,t) + \mathbf{f}(\mathbf{u}(x,t)) \frac{\partial}{\partial x}\varphi(x,t) \right\} \mathrm{d}x\mathrm{d}t = - \int_{-\infty}^\infty \mathbf{u}^0(x)\varphi(x,0)\mathrm{d}x - \int_0^\infty \int_{-\infty}^\infty \mathbf{q}(\mathbf{u}(x,t))\varphi(x,t)\mathrm{d}x\mathrm{d}t \tag{2.3}$$

for all functions $\varphi \in C_0^1(I\!R \times [0,\infty))$.

From now on by a solution of (2.2) a weak solution of (2.2) in the sense of Definition 2.1 is meant. It can be shown that a solution of (2.1) is always a weak solution of (2.2).

A difficulty is that the weak solutions of (2.2) turn out to be nonunique for a given set of initial data, and it remains to characterise the "physically relevant" weak solution. The usual criterion is to impose an extra condition upon the solution, the so-called entropy condition, such that a physically relevant solution is obtained [7].

The system (2.2a) is assumed to be hyperbolic, i.e. the Jacobian matrix of $\mathbf{f}(\mathbf{u})$, defined by $A(\mathbf{u}) = \frac{\partial}{\partial \mathbf{u}}\mathbf{f}(\mathbf{u})$, has real eigenvalues and m linearly independent eigenvectors. A very important example of a system of hyperbolic conservation laws with source terms are the reactive Euler equations [3, 4, 10], which are described in the next section. In Section 4 we describe a simplified detonation model which serves as a second example.

3 The Reactive Euler Equations

3.1 Introduction

Consider a tube filled with a gas mixture that is uniformly distributed across the tube, so there is variation in only one direction and we can restrict ourselves to one space dimension. For the sake of simplicity we assume that the gas is a binary mixture in which only one chemical reaction takes place. Thus consider the one-step reaction "unburnt gas $\rightarrow$ burnt gas". Further assume that a detonation wave is propagating in the positive x-direction. All quantities ahead of the detonation wave will be identified by the subscript u (the unburnt gas), while the quantities behind the wave are denoted by the subscript b (the burnt gas).

For detonation waves the general combustion equations simplify to the reactive Euler equations. These equations represent the conservation of mass, momentum and energy of the total mixture and the balance of mass for the unburnt gas. The latter equation includes a source term describing the one-step chemical reaction. With mass density ρ, mass weighted average velocity u, pressure p, specific total energy E, mass fraction of the unburnt gas Y and reaction rate w, the one-dimensional reactive Euler equations are

$$\frac{\partial}{\partial t}(\rho) + \frac{\partial}{\partial x}(\rho u) = 0, \tag{3.1a}$$

$$\frac{\partial}{\partial t}(\rho u) + \frac{\partial}{\partial x}(\rho u^2 + p) = 0, \tag{3.1b}$$

$$\frac{\partial}{\partial t}(\rho E) + \frac{\partial}{\partial x}(\rho u E + p u) = 0, \tag{3.1c}$$

$$\frac{\partial}{\partial t}(\rho Y) + \frac{\partial}{\partial x}(\rho u Y) = w. \tag{3.1d}$$

All variables have been made dimensionless by normalising them with respect to some reference state. To complete the system (3.1), the pressure p and the reaction rate w have to be related to the independent variables ρ, u, E and Y. If we assume that both gases behave like an ideal gas with the same specific heat ratio γ, then the thermodynamic identity is given by

$$p = (\gamma - 1)\rho(E - \frac{1}{2}u^2 - QY), \tag{3.2}$$

where $Q > 0$ is the specific heat release of the chemical reaction. In general the reaction rate w depends on the temperature T via some Arrhenius relation [3, 5, 10]. Typically the reaction rate is very large when the temperature is sufficiently high but negligible for small T. For simplicity we can approximate this by an 'ignition temperature' kinetics model, in which the Arrhenius behaviour is idealised to [3]

$$w = \begin{cases} 0, & T < T_{ign}, \\ -Da\,\rho Y, & T \geq T_{ign}, \end{cases} \tag{3.3}$$

where T_{ign} is the ignition temperature and Da is referred to as the Damköhler number. The ignition temperature satisfies $T_u < T_{ign} \leq T_{vN}$, where T_{vN} is the von Neumann temperature, which is discussed in Section 3.3. The Damköhler number is defined as the ratio of the convection time scale and the reaction time scale [10]. Obviously, if Da is small the reaction occurs slowly relative to the specified time scale and if Da is large, the reaction zone is thin and the reaction occurs quickly relative to the specified time scale. Equation (3.3) defines w as a function of ρ, u, E and Y through the thermodynamic identity (3.2) and the equation of state

$$p = \rho T. \tag{3.4}$$

The system of equations (3.1), (3.2), (3.3) and (3.4) consists of seven equations for the variables ρ, u, E, Y, p, T and w.

In this paper a short description is given of two well-known models for detonation waves, namely the Chapman-Jouguet model and the ZND model.

3.2 The Chapman-Jouguet Model

If the Damköhler number Da is very large, then the reaction length is very small relative to the convection length. We start with considering the limit $Da \to \infty$, in which case the gas is burnt instantaneously. We then expect that across a combustion wave the state variables will be discontinuous. The temperature will jump to a higher value and Y will jump from 1 to 0. From conservation of mass, momentum and energy a set of allowable jumps and associated shock speeds can be determined analogously to the derivation of the Rankine-Hugoniot conditions for ordinary shock waves. The corresponding equations are called the reactive Rankine-Hugoniot equations.

For details concerning these equations the reader is referred to e.g. [4, 5, 10]. In this paper we just summarise some results obtained from the reactive Rankine-Hugoniot equations. If a detonation wave passes the unburnt gas, the pressure and the density jump to higher values, i.e. $p_b > p_u$ and $\rho_b > \rho_u$. Detonation waves can be distinguished in three different types, namely strong, Chapman-Jouguet and weak detonation waves. We present, without proof, some characteristic properties by which we can distinguish the various detonation waves. These properties are referred to as Jouguet's rule [4].

Jouguet's Rule:
The gas flow relative to the reaction front is

supersonic ahead of a detonation front (i.e. $s - u_u > c_u$),

subsonic behind a strong detonation front (i.e. $0 < s - u_b < c_b$),

sonic behind a Chapman-Jouguet detonation front (i.e. $s - u_b = c_b$),

supersonic behind a weak detonation front (i.e. $s - u_b > c_b$),

where $c = \sqrt{\gamma p/\rho}$ is the speed of sound and s is the speed of the detonation wave. The Chapman-Jouguet (CJ) detonation wave is of particular importance since this wave travels with the minimal speed of all the possible detonation waves. Note that practically all detonation waves observed in nature travel at approximately the CJ velocity. Finally, it can be shown that weak detonations are only possible under extreme and rare circumstances [4].

3.3 The ZND Model

The previous considerations give no insight into the internal structure of detonation waves, since Da was assumed to be infinitely large. For finite Damköhler numbers we expect some region of finite width across which the reaction takes place. Independently from each other, Zel'dovich, von Neumann and Döring developed a model that explains the internal structure of detonation waves, the so-called ZND model [4, 5, 10]. The ZND model assumes the following.

> *A detonation wave travelling with constant speed s has the internal structure of an ordinary (nonreacting) precursor fluid dynamical shock wave followed by a reaction zone.*

Hence, due to a strong leading shock wave the temperature of the unburnt gas T_u jumps to a value larger than T_{ign} and a reaction is started. The values immediately behind the nonreacting shock wave are called the von Neumann values and are the final values if no chemical reaction takes place. For instance, the temperature behind the ordinary shock wave is called the von Neumann temperature T_{vN}. As the reaction proceeds (through the reaction zone) Y decreases from 1 to 0 and the pressure and density decrease to their final values p_b and ρ_b, respectively. Suppose all states ahead of the detonation wave are known. For given Q, γ, Da and s we can compute the exact ZND solution of (3.1). An example of a ZND profile is given in Figure 1. In this figure the ordinary shock wave is located at $x = 0$. Finally, it is convenient to introduce the half reaction length $L_{1/2}$. The half reaction length is the distance for half completion of the reaction starting from the front of the detonation wave [2]. Often $L_{1/2}$ is given and (3.3) is used to compute the corresponding Damköhler number Da.

Example 3.1 As an example of the preceding theory we describe the ZND solution of a strong detonation. All quantities are nondimensionalised with respect to the unburnt gas. Hence, the dimensionless preshock state is given by

$$p_u = 1, \qquad \rho_u = 1, \qquad u_u = 0.$$

Furthermore, we have the following parameter values:

$$Q = 10, \qquad \gamma = 1.4, \qquad Da = 6.7486,$$

which implies that $L_{1/2} = 0.1$. We choose a relatively small Da, since otherwise the reaction is very fast and the plot of the ZND profile is not very clarifying. The final state for the strong detonation is given by

$$p_b = 14.489, \qquad \rho_b = 2.1718, \qquad u_b = 2.6977,$$

where the strong detonation is propagating with a speed $s = 5$. In Figure 1 the steady ZND solution is drawn. The pressure reaches its maximum value right behind the precursor shock. The pressure in this point is called the von Neumann pressure, which in this particular case satisfies $p_{vN} = 20.667$. For this particular example the von Neumann temperature is given by $T_{vN} = 4.4089$.

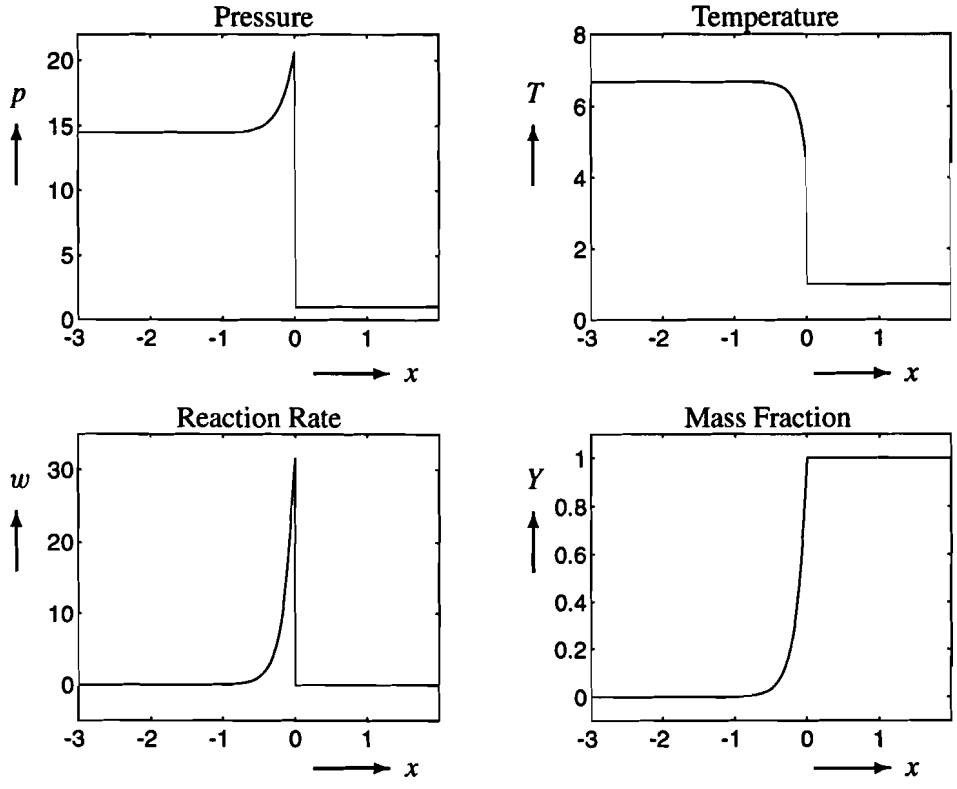

Figure 1: Strong detonation as described by the ZND model, with $Q = 10$, $\gamma = 1.4$ and $Da = 6.7486$.

4 A Simplified Detonation Model

4.1 Introduction

Even in one space variable the reactive Euler equations (3.1) are complicated, so it is not surprising that simpler qualitative models for the equations (3.1) have been developed. Although physically not very realistic, these model problems are interesting for testing and analysing numerical methods. Clearly, simplified models are inadequate as full test problems for any numerical method. However, a study of these problems suffices to analyse some of the difficulties that may arise in the more complicated systems.

The model of interest bears the analogous relationship to the reactive Euler equations as Burgers' equation does to the ordinary Euler equations. This model is the 2×2 system of equations

$$\frac{\partial}{\partial t}u + \frac{\partial}{\partial x}(\tfrac{1}{2}u^2) = -Qw(u, Y), \tag{4.1a}$$

$$\frac{\partial}{\partial t}Y = w(u, Y). \tag{4.1b}$$

In the above model Y plays a similar role as the mass fraction of the unburnt gas and $Q > 0$ can be interpreted as the heat release of the chemical reaction. Analogously to (3.3), the reaction rate w is given by

$$w(u, Y) = \begin{cases} 0, & u < u_{ign}, \\ -Da\, Y, & u \geq u_{ign}, \end{cases} \tag{4.2}$$

where u_{ign} is the ignition value of the chemical reaction and Da is referred to as the Damköhler number. Analogously to (3.3) we refer to u_{ign} as the ignition temperature, although it represents not a specific temperature. The above model problem (4.1) is called the simplified detonation model. We emphasise that (4.1) is only used as a numerical test problem and has no real physical meaning. A physically more realistic test problem is obtained when $\partial Y/\partial t$ is replaced by $\partial Y/\partial x$ [3]. However, we have experienced that for testing and analysing numerical methods the numerical behaviour of (4.1) is more similar to that of the reactive Euler equations.

Note that if $\mathbf{u}$, $\mathbf{f}(\mathbf{u})$ and $\mathbf{q}(\mathbf{u})$ are defined by, respectively,

$$\mathbf{u} = (u\,,\, Y)^T, \qquad \mathbf{f}(\mathbf{u}) = (\tfrac{1}{2}u^2\,,\, 0)^T, \qquad \mathbf{q}(\mathbf{u}) = (-Qw\,,\, w)^T, \tag{4.3}$$

then the simplified detonation model (4.1) can be written in the general form (2.2a). For a detailed description of this model problem, see [9]. For (4.1) we can develop a theory which has similar features as the theory presented in Section 3.2 and 3.3. We start with the analogue of the Chapman-Jouguet model.

4.2 The Analogue of the Chapman-Jouguet Model

Again we start with considering the limit $Da \to \infty$, i.e. the gas is burnt instantaneously. We assume that a travelling wave is propagating with a constant velocity $s > 0$ in the positive x-direction. Analogously to reacting gas dynamics we call this wave a detonation wave. Furthermore, it is assumed that the flow is steady with respect to a coordinate system moving with the detonation wave. All quantities ahead of the detonation wave will again be identified by the subscript u (the unburnt gas), while the quantities behind the wave are denoted by the subscript b (the burnt gas). The variable ξ is introduced as $\xi(x, t) = x - st$ and subsequently, (4.1) can be rewritten as a system of ordinary differential equations, i.e.

$$-s\frac{\mathrm{d}}{\mathrm{d}\xi}u + \frac{\mathrm{d}}{\mathrm{d}\xi}(\tfrac{1}{2}u^2) = -Qw(u, Y), \tag{4.4a}$$

$$-s\frac{\mathrm{d}}{\mathrm{d}\xi}Y = w(u, Y). \tag{4.4b}$$

We assume that u and Y satisfy

$$\lim_{\xi \to \infty}(u(\xi), Y(\xi)) = (u_u, 1), \tag{4.5a}$$

$$\lim_{\xi \to -\infty}(u(\xi), Y(\xi)) = (u_b, 0), \tag{4.5b}$$

where $u_u + Q < u_b$ and $0 \leq u_u < u_{ign} \leq u_b$. After integrating (4.4a) from $\xi = -\infty$ to $\xi = +\infty$ and using (4.5) we deduce

$$s(u_b - u_u - Q) = \tfrac{1}{2}u_b^2 - \tfrac{1}{2}u_u^2. \tag{4.6}$$

Consistently to the reactive Euler equations the above equation is called the reactive Rankine-Hugoniot equation. For details the reader is referred to e.g. [9].

Analogously to Section 3.2 we can distinguish three different types of detonation waves, namely strong, Chapman-Jouguet and weak detonation waves. We replace u_b by u_{st}, u_{CJ} or u_{we} in case of a strong, Chapman-Jouguet or weak detonation, respectively. It can be shown, using (4.6), that $s_{CJ} > 0$ is given by

$$s_{CJ} = u_u + Q + \sqrt{Q^2 + 2u_u Q}. \tag{4.7}$$

For all $s < s_{CJ}$ there will be no detonation. If $s = s_{CJ}$, then there will be a CJ detonation with

$$u_{CJ} = s_{CJ} = u_u + Q + \sqrt{Q^2 + 2u_u Q}. \tag{4.8}$$

If $s > s_{CJ}$, then there will be a detonation with

$$u_{st} = s + \sqrt{(s - u_u)^2 - 2sQ}, \tag{4.9}$$

in case of a strong detonation or

$$u_{we} = s - \sqrt{(s - u_u)^2 - 2sQ}, \tag{4.10}$$

in case of a weak detonation. Finally, detonation waves can be distinguished by the following characteristic properties.

For detonation waves $s > u_u$,

For strong detonations $s < u_{st} = u_b$,

For Chapman-Jouguet detonations $s = s_{CJ} = u_b$,

For weak detonations $s > u_{we} = u_b$.

The above properties are the analogue for Jouguet's rule. Again the only relevant detonations are Chapman-Jouguet and strong detonations.

4.3 The Analogue of the ZND Model

Next we briefly develop the analogue for the ZND theory, as described in Section 3.3. Again we assume that a detonation wave travelling with constant speed s has the internal structure of an ordinary (nonreacting) precursor shock wave followed by a reaction zone. Hence the front of a detonation wave is a shock wave that initiates a chemical reaction behind it.

Firstly, due to a shock wave the variable u jumps to a higher value, called, analogously to reactive gas dynamics, the von Neumann spike (vN-spike). It is straightforward that $u_{vN} = 2s - u_u$, and subsequently,

$$u_u < s < u_{vN}.$$

The von Neumann spike is the state immediately behind the shock wave and is the final state if no reaction takes place. It is clear that $u_{vN} > u_b \geq u_{ign}$. As the reaction proceeds Y decreases from 1 to 0 and the u decreases to the final value u_b.

It can be shown that for the ZND model the final state is a strong or CJ detonation. The minimum speed for a detonation wave is the speed s_{CJ} of a CJ detonation. It will be useful to define a quantity which measures the overdrive of a strong detonation. Therefore, let the degree of overdrive f be defined by [2]

$$f = (s/s_{CJ})^2, \tag{4.11}$$

from which it directly follows that $f \geq 1$. Suppose that all states ahead of the detonation wave are known, i.e. u_u is given and $Y_u = 1$. Furthermore the parameters u_{ign}, Da, f and Q are known. Firstly we compute the speed s_{CJ} of a CJ detonation using (4.7). Using the degree of overdrive f we can compute the detonation speed as $s = s_{CJ}\sqrt{f}$. Using (4.8), (4.9) or (4.10) we can compute the final state of the detonation wave. An example of a ZND profile is given in Figure 2. Finally, the half reaction length $L_{1/2}$ is introduced as the distance for half completion of the reaction starting from the front of the detonation wave. It this case $L_{1/2}$ is given by

$$L_{1/2} = \frac{s}{Da}\ln(2).$$

Often $L_{1/2}$ is given and the previous relation is used to compute the corresponding Damköhler number Da.

Example 4.1 As an example of the preceding theory we describe the ZND solution of the strong detonation with

$$u_u = 0, \qquad Q = 2, \qquad f = 1.265625, \qquad Da = 31.192.$$

The half reaction length is given by $L_{1/2} = 0.1$. The final state for the strong detonation is given by $u_b = 6$, where the detonation is propagating with a speed $s = 4.5$. In Figure 2 the steady ZND solution is drawn. The variable u reaches its maximum value right behind the precursor shock. As mentioned before this value is called the von Neumann spike, which in this particular case satisfies $u_{vN} = 9$.

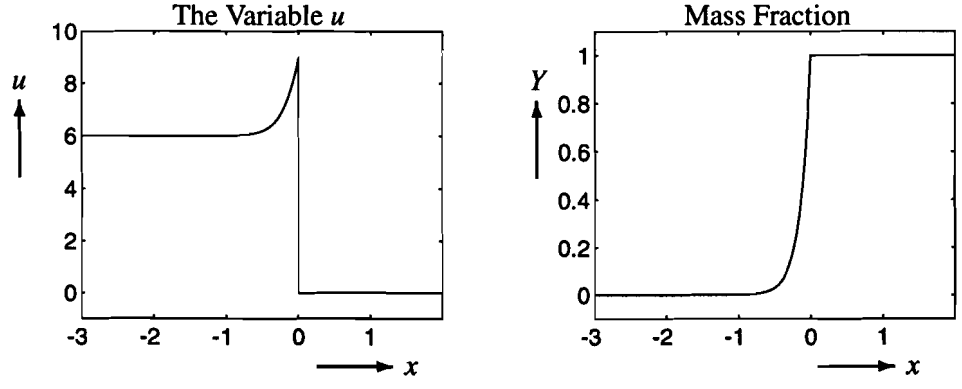

Figure 2: ZND solution of (4.1) with $Q = 2$, $f = 1.265625$ and $Da = 31.192$.

5 The Numerical Computation of Strong or CJ Detonation Waves for the Simplified Detonation Model

In this section we want to compute strong or CJ detonation waves propagating with a constant wave speed $s > 0$, as described in Section 4. For the sake of simplicity we assume that the initial data $\mathbf{u}^0$ are given by

$$(u^0(x), Y^0(x))^T = \begin{cases} (u_b, 0)^T, & x < 0, \\ (u_u, 1)^T, & x > 0. \end{cases} \tag{5.1}$$

Hence, at time $t = 0$ only burnt gas is present at the left-hand side of $x = 0$ and only unburnt gas is present at the right-hand side of $x = 0$ (see (4.5)). .

In the remainder it is assumed that u_b is the final state of a strong or CJ detonation wave propagating with a constant wave speed $s > 0$.

A variety of numerical methods can be developed for conservation laws with source terms. A very natural way to solve (4.1) is a first order splitting method. In the splitting method the numerical solution at each time level is derived by a two-step procedure. In the first step we assume that no reaction occurs (i.e. $w = 0$ in (4.1)) and approximate the solution of the remaining homogeneous equation, i.e. Burgers' equation. In the second step we assume no convection (i.e. $\partial u^2/\partial x = 0$ in (4.1)) and solve the corresponding ordinary differential equations numerically. There are several reasons for studying first order splitting methods. Firstly the splitting method is interesting since good numerical methods exist for both subproblems. Furthermore, this method lends itself for thorough analysis. Finally second order accuracy can be achieved using the Strang splitting [3].

For a given time step Δt the discrete time levels t^n are defined by

$$t^n = n\Delta t, \quad n = 0, 1, 2, \ldots .$$

For a given mesh width Δx the spatial mesh points x_i are defined by

$$x_i = i\Delta x, \quad i = \ldots, -2, -1, 0, 1, 2, \ldots .$$

It will also be useful to define intermediate points

$$x_{i+1/2} = (i + \tfrac{1}{2})\Delta x.$$

The finite difference method we shall consider, produces approximations $\mathbf{U}_i^n \in I\!R^2$ to the true solution $\mathbf{u}(x_i, t^n)$. The average of $\mathbf{u}(\cdot, t^n)$ over the cell $[x_{i-1/2}, x_{i+1/2})$ is defined by

$$\bar{\mathbf{u}}_i^n = \frac{1}{\Delta x} \int_{x_{i-1/2}}^{x_{i+1/2}} \mathbf{u}(x, t^n) \mathrm{d}x. \tag{5.2}$$

For conservation laws it is often convenient to consider $\mathbf{U}_i^n$ as an approximation to this average, since the integral form (2.1) of the conservation law describes the evolution in time of integrals as (5.2). In the following it is assumed that, for a given constant $\tau > 0$, the mesh width Δx and time step Δt satisfy

$$\frac{\Delta t}{\Delta x} = \tau.$$

For the sake of convenience, we construct a piecewise constant function $\mathbf{U}_{\Delta t}(\cdot, t^n)$ from the discrete values $\mathbf{U}_i^n$ by

$$\mathbf{U}_{\Delta t}(x, t^n) = \mathbf{U}_i^n, \quad \forall x \in [x_{i-1/2}, x_{i+1/2}). \tag{5.3}$$

In the first step we have to approximate the solution of Burgers' equation (the mass fraction Y remains constant during the first step). We use Roe's conservative three-point method. For later purposes it will be useful to denote the result by C_i^n, so

$$C_i^n = U_i^n - \tau\{F_{i+1/2}^n - F_{i-1/2}^n\}, \tag{5.4}$$

where the numerical flux function F is given by

$$F_{i+1/2}^n = F(U_i^n, U_{i+1}^n) = \begin{cases} \frac{1}{2}(U_{i+1}^n)^2, & U_i^n + U_{i+1}^n < 0, \\ \frac{1}{2}(U_i^n)^2, & U_i^n + U_{i+1}^n > 0. \end{cases} \tag{5.5}$$

If the second step (the reactive step) is solved by the backward Euler method, then the total finite difference scheme reads

$$U_i^{n+1} = U_i^n - \tau\{F_{i+1/2}^n - F_{i-1/2}^n\} - \Delta t Q w(U_i^{n+1}, Y_i^{n+1}), \tag{5.6a}$$

$$Y_i^{n+1} = Y_i^n + \Delta t w(U_i^{n+1}, Y_i^{n+1}). \tag{5.6b}$$

As usual, the time step Δt is restricted by the CFL stability condition, i.e. $\tau \max_i |U_i^n| \leq 1$.

When attempting to solve (4.1) numerically, it is possible to obtain stable numerical solutions that seem reasonable and yet are completely wrong, since the numerical solution approximates a nonphysical weak solution. In order to study this problem we define two quantities S_1^n and S_2^n at time t^n by

$$S_1^n n \Delta t (u_b - u_u) = \Delta x \sum_{i=-\infty}^{\infty} \left(U_i^n - U_i^0\right), \tag{5.7a}$$

$$-S_2^n n \Delta t = \Delta x \sum_{i=-\infty}^{\infty} \left(Y_i^n - Y_i^0\right). \tag{5.7b}$$

Since $\mathbf{u}^0$ is constant outside some finite interval (see (5.1)) so is $\mathbf{U}_i^n$, because method (5.6) has a finite domain of dependence. Hence, the right-hand side of (5.7) is finite and S_1^n and S_2^n are well defined. The quantity S_2^n can be interpreted as the average speed of the numerical detonation wave. Normally the numerical wave speed for a finite difference method is given by an expression of the form $m\Delta x/(l\Delta t)$, where l and m are relatively prime numbers. In other words, the numerical solution propagates m spatial grid points for every l time steps. However, in general m and l are hard to compute from the numerical results. On the other hand, S_1^n and S_2^n can be computed easily by (5.7).

The following theorem gives a relation between S_1^n and S_2^n, which is the numerical analogon of the reactive Rankine-Hugoniot relation (4.6).

Theorem 5.1 *Suppose that the finite difference method* (5.6) *is used to approximate the simplified detonation model* (4.1) *with initial data that satisfy* (5.1). *Let* $\mathbf{U}_i^n = (U_i^n, Y_i^n)^T$ *be a solution of* (5.6) *with given initial values* $\mathbf{U}_i^0 = \bar{\mathbf{u}}_i^0$, *as defined in* (5.2). *Then* S_1^n *and* S_2^n *satisfy the relation*

$$S_1^n(u_b - u_u) - S_2^n Q = \tfrac{1}{2}u_b^2 - \tfrac{1}{2}u_u^2. \tag{5.8}$$

Proof Since the first step of the splitting method is explicit, it follows from (5.1) that

$$\lim_{i \to -\infty} F_{i-1/2}^n = \tfrac{1}{2}u_b^2 \quad \text{and} \quad \lim_{i \to \infty} F_{i+1/2}^n = \tfrac{1}{2}u_u^2,$$

for all $n \geq 0$. We start with replacing $n+1$ by j in (5.6). After multiplying the resulting scheme by Δx, summing over i and using the above limits we obtain

$$\Delta x \sum_{i=-\infty}^{\infty} \left(U_i^j - U_i^{j-1}\right) = \Delta t \left\{\tfrac{1}{2}u_b^2 - \tfrac{1}{2}u_u^2\right\} - \Delta t \Delta x\, Q \sum_{i=-\infty}^{\infty} w(U_i^j, Y_i^j),$$

$$\Delta x \sum_{i=-\infty}^{\infty} \left(Y_i^j - Y_i^{j-1}\right) = \Delta t \Delta x \sum_{i=-\infty}^{\infty} w(U_i^j, Y_i^j).$$

Summing the above equations over all j with $1 \leq j \leq n$, we see that

$$\Delta x \sum_{i=-\infty}^{\infty} \left(U_i^n - U_i^0\right) = n\Delta t \left\{\tfrac{1}{2}u_b^2 - \tfrac{1}{2}u_u^2\right\} - \Delta t \Delta x\, Q \sum_{j=1}^{n} \sum_{i=-\infty}^{\infty} w(U_i^j, Y_i^j),$$

$$\Delta x \sum_{i=-\infty}^{\infty} \left(Y_i^n - Y_i^0\right) = \Delta t \Delta x \sum_{j=1}^{n} \sum_{i=-\infty}^{\infty} w(U_i^j, Y_i^j).$$

After substituting the second equation into the first and, subsequently, replacing the summations using (5.7), it follows that

$$S_1^n n\Delta t(u_b - u_u) = n\Delta t \left\{\tfrac{1}{2}u_b^2 - \tfrac{1}{2}u_u^2\right\} + S_2^n n\Delta t Q.$$

After dividing the latter equation by $n\Delta t$ the result (5.8) follows immediately. This completes the proof. □

Remember that the correct solution of (4.1)-(5.1) is assumed to be a strong or CJ detonation wave propagating with constant speed $s > 0$. As noted before, for large Da it is possible to obtain numerical solutions that approximate a nonphysical weak solution of (4.1). This wrong solution appears to be a weak detonation wave followed by an ordinary shock wave (see Figure 6). In order to approximate the correct weak solution, the final state of the burnt gas directly behind the numerical detonation wave should be equal to u_b as $n \to \infty$. Let $v_b^n > 0$ be given such that

$$S_2^n(v_b^n - u_u - Q) = \tfrac{1}{2}(v_b^n)^2 - \tfrac{1}{2}u_u^2, \tag{5.9}$$

where it is assumed that $S_2^n \geq s_{CJ}$, since otherwise v_b^n will not exist (see Section 4). Furthermore, it follows from $v_b^n > 0$, $S_2^n > 0$ and (5.9) that $v_b^n > u_u + Q$. The constant v_b^n is the final state of a detonation wave propagating with speed S_2^n. If $S_2^n > s_{CJ}$, there are two possible values for v_b^n such that (5.9) is satisfied, namely: $v_b^n > S_2^n$ in case of a strong detonation and $v_b^n < S_2^n$ in case of a weak detonation. The wrong weak solutions mentioned above, consists of a detonation wave linking the state $(u_u, 1)^T$ to $(v_b^n, 0)^T$, followed by an ordinary shock wave linking the states $(v_b^n, 0)^T$ and $(u_b, 0)^T$. Let $\bar{S}^n$ denotes the speed of this shock wave, i.e.

$$\bar{S}^n = \tfrac{1}{2}(v_b^n + u_b). \tag{5.10}$$

The existence of numerical solutions that approximate this nonphysical weak solution is illustrated by the following theorem.

Theorem 5.2 *Suppose that all the assumptions of Theorem 5.1 hold and let* $\mathbf{U}_{\Delta t} = (U_{\Delta t}, Y_{\Delta t})^T$ *be given by* (5.3). *Furthermore, let* $n > 0$ *and assume that* $S_2^n \geq s_{CJ}$, *i.e. there exists a* v_b^n *such that* (5.9) *holds. Finally, the function* $\tilde{\mathbf{u}}^n(\cdot, t^n)$ *is defined by*

$$\tilde{\mathbf{u}}^n(x, t^n) = \begin{cases} (u_b, 0)^T, & x < \bar{S}^n t^n, \\ (v_b^n, 0)^T, & \bar{S}^n t^n < x < S_2^n t^n, \\ (u_u, 1)^T, & x > S_2^n t^n. \end{cases} \tag{5.11}$$

Then

$$\int_{-\infty}^{\infty} (\mathrm{U}_{\Delta t}(x, t^n) - \tilde{\mathbf{u}}^n(x, t^n))\mathrm{d}x \;=\; \mathbf{0}. \tag{5.12}$$

Furthermore, for given S_2^n and v_b^n such that (5.9) *holds, $\tilde{\mathbf{u}}^n(\cdot, t^n)$ is the only piecewise constant function consisting of maximal three constant states $(c_1, 0)^T$, $(c_2, 0)^T$ and $(c_3, 1)^T$, such that* (5.12) *holds.*

Hence, we have discrete conservation with respect to the solution $\tilde{\mathbf{u}}^n$ given in (5.11). Suppose that the numerical solution consists of three constant states $(c_1, 0)^T$, $(c_2, 0)^T$ and $(c_3, 1)^T$, then Theorem 5.2 implies that any shocks we compute at time t^n must, in a sense, have the same location as the shocks in $\tilde{\mathbf{u}}^n$. Note that (5.11) consists of a detonation wave followed by an ordinary shock wave. Thus, $\tilde{\mathbf{u}}^n$ is the nonphysical weak solution that is observed in our numerical experiments. Furthermore, we remark that if $v_b^n = u_b$, then $S_2^n = s$ and (5.11) is the physically correct weak solution.

Proof Since $\mathbf{u}^0$ is piecewise constant and explicit methods have finite domain of dependence, $\mathrm{U}_{\Delta t}$ is constant outside some finite interval. Furthermore, since (5.6) is three-point method, initial data (5.1) are used, $\bar{S}^n > 0$ and $S_2^n < \Delta x/\Delta t$,

$$\int_{-\infty}^{\infty} (\mathrm{U}_{\Delta t}(x, t^n) - \tilde{\mathbf{u}}^n(x, t^n))\,\mathrm{d}x \;=\; \int_{-(n+1/2)\Delta x}^{(n+1/2)\Delta x} (\mathrm{U}_{\Delta t}(x, t^n) - \tilde{\mathbf{u}}^n(x, t^n))\,\mathrm{d}x. \tag{5.13}$$

Note that (5.12) consists of two equations, one equation for U and one equation for Y. Firstly we proof the second equality in (5.12). After replacing the summation in (5.7b) by an integral, using (5.3), and subsequently applying (5.13), we arrive at

$$\int_{-(n+1/2)\Delta x}^{(n+1/2)\Delta x} Y_{\Delta t}(x, t^n)\,\mathrm{d}x \;=\; (n + \tfrac{1}{2})\Delta x \;-\; S_2^n t^n. \tag{5.14}$$

Now the second equation in (5.12) follows directly from (5.11), (5.13) and (5.14). Analogously, we replace the summation in (5.7a) by an integral and obtain, using (5.1) and (5.13),

$$\int_{-(n+1/2)\Delta x}^{(n+1/2)\Delta x} U_{\Delta t}(x, t^n)\,\mathrm{d}x \;=\; (n + \tfrac{1}{2})\Delta x u_b \;+\; S_1^n t^n(u_b - u_u) \;+\; (n + \tfrac{1}{2})\Delta x u_u. \tag{5.15}$$

Using (4.6), (5.8), (5.9) and (5.10), we obtain

$$\begin{aligned} S_1^n t^n(u_b - u_u) &= st^n(u_b - u_u - Q) + S_2^n t^n Q \\ &= t^n(\tfrac{1}{2}u_b^2 - \tfrac{1}{2}(v_b^n)^2) + t^n(\tfrac{1}{2}(v_b^n)^2 - \tfrac{1}{2}u_u^2) + S_2^n t^n Q \\ &= \bar{S}^n t^n(u_b - v_b^n) + S_2^n t^n(v_b^n - u_u). \end{aligned}$$

Using this together with (5.11) and (5.15) gives

$$\begin{aligned}\int_{-(n+1/2)\Delta x}^{(n+1/2)\Delta x} U_{\Delta t}(x,t^n)\,dx &= (n+\tfrac{1}{2})\Delta x u_b + \bar{S}^n t^n u_b + (S_2^n - \bar{S}^n)t^n v_b^n \\ &\quad + ((n+\tfrac{1}{2})\Delta x - S_2^n t^n)u_u \\ &= \int_{-(n+1/2)\Delta x}^{(n+1/2)\Delta x} \tilde{u}^n(x,t^n)\,dx.\end{aligned}$$

This completes the proof of (5.12). It remains to proof that $\tilde{\mathbf{u}}^n(\cdot,t^n)$ is the only piecewise constant function consisting of maximal three constant states, such that (5.12) holds. It follows from (5.1) that two constant states are given by $(u_u,1)^T$ and $(u_b,0)^T$. Denote the third constant state by $(c,0)^T$ and let the function $\tilde{\mathbf{w}}^n(\cdot,t^n) = (\tilde{w}_1^n(\cdot,t^n), \tilde{w}_2^n(\cdot,t^n))^T$ be given by

$$\tilde{\mathbf{w}}^n(x,t^n) = (\tilde{w}_1^n(x,t^n), \tilde{w}_2^n(x,t^n))^T = \begin{cases} (u_b,0)^T, & x < a, \\ (c,0)^T, & a < x < b, \\ (u_u,1)^T, & x > b, \end{cases} \tag{5.16}$$

where $0 < a \le b$. We have to show that $a = \bar{S}^n t^n$, $b = S_2^n t^n$ and $c = v_b^n$ (see (5.11)). It follows from (5.14) and (5.16) that $b = S_2^n t^n$. Since $\tilde{\mathbf{w}}^n$ satisfies (5.12) and (5.13) holds, it follows from (5.15) and $a = \frac{1}{2}(u_b + c)t^n$ that

$$\begin{aligned}\int_{-(n+1/2)\Delta x}^{(n+1/2)\Delta x} (U_{\Delta t}(x,t^n) - \tilde{w}_2^n(x,t^n))\,dx &= S_1^n t^n(u_b - u_u) + a(c - u_b) + S_2^n t^n(u_u - c) \\ &= S_2^n t^n Q + t^n(\tfrac{1}{2}u_b^2 - \tfrac{1}{2}u_u^2) + t^n(\tfrac{1}{2}c^2 - \tfrac{1}{2}u_b^2) \\ &\quad + S_2^n t^n(u_u - c) \\ &= S_2^n t^n(-c + u_u + Q) + t^n(\tfrac{1}{2}c^2 - \tfrac{1}{2}u_u^2) \\ &= 0.\end{aligned}$$

The last equality and (5.9) imply that $c = v_b^n$ and, subsequently $a = \bar{S}^n t^n$. This completes the proof. □

The main goal of this section is to derive a criterion that excludes nonphysical weak solutions. In other words, we want to exclude numerical approximations of (5.11), except for the case $v_b^n = u_b$ and $S_2^n = s$. First of all, we remark that numerical experiments show that the sequence S_2^n always converges as $n \to \infty$. Therefore, we assume that there exists a positive constant S_2 such that $\lim_{n\to\infty} S_2^n = S_2$. It follows from (5.9) that $\lim_{n\to\infty} v_b^n = v_b$ for some v_b and subsequently, S_2 and v_b are related by

$$S_2(v_b - u_u - Q) = \tfrac{1}{2}v_b^2 - \tfrac{1}{2}u_u^2. \tag{5.17}$$

An important question is whether the piecewise constant solution (5.11) is stable as time evolves. Here by stability is meant that $\tilde{\mathbf{u}}^n$ remains (as n increases) a piecewise constant function consisting of the three constant states $(u_u,1)^T$, $(v_b^n,0)^T$ and $(u_b,0)^T$ such that $\lim_{n\to\infty} v_b^n = v_b$. This is important since an apparently wrong solution $\tilde{\mathbf{u}}^n$ might converge to the correct weak solution as $n \to \infty$. For convenience sake, we replace v_b^n, S_2^n and $\bar{S}^n$ in (5.11) by the corresponding limit values, v_b, S_2 and $\bar{S} = \frac{1}{2}(v_b + u_b)$.

Theorem 5.3 *Let u_u, s and S_2 be given and assume that u_b is the final state of a strong or CJ detonation wave propagating with speed s and v_b is the final state of a detonation wave propagating with speed S_2, i.e.* (4.6) *and* (5.17) *hold. Suppose that the initial data* $\mathbf{u}^0$ *are given by (see* (5.11)*)*

$$(u^0(x), Y^0(x))^T = \begin{cases} (u_b, 0)^T, & x < a, \\ (v_b, 0)^T, & a < x < b, \\ (u_u, 1)^T, & x > b, \end{cases} \tag{5.18}$$

where $a < b$ are given constants. Let $\mathbf{u} = (u, Y)^T$ *be a weak solution of* (4.1) *with initial data* (5.18) *and suppose that* $\mathbf{u}$ *consists of at most three constant states for all t. Then for t sufficiently large,*

(i) *if $v_b > u_{we}$, then the weak solution* $\mathbf{u}$ *consist of two constant states separated by a strong or CJ detonation wave, i.e. $v_b = u_b$, propagating with a speed $S_2 = s$, i.e.*

$$\mathbf{u}(x,t) = (u(x,t), Y(x,t))^T = \begin{cases} (u_b, 0)^T, & x < d + st, \\ (u_u, 1)^T, & x > d + st, \end{cases} \tag{5.19}$$

for some constant $d > a$;

or,

(ii) *if $v_b \leq u_{we}$, then the weak solution* $\mathbf{u}$ *consist of a weak detonation wave propagating with speed $S_2 \geq s$, followed by an ordinary shock wave propagating with speed $\bar{S} = (u_b + v_b)/2 < s$, i.e.*

$$\mathbf{u}(x,t) = (u(x,t), Y(x,t))^T = \begin{cases} (u_b, 0)^T, & x < a + \bar{S}t, \\ (v_b, 0)^T, & a + \bar{S}t < x < b + S_2 t, \\ (u_u, 1)^T, & b + S_2 t < x. \end{cases} \tag{5.20}$$

Here u_{we} denotes the final state of the weak detonation propagating with speed s (see (4.10)*).*

Note that if $v_b = u_b$ and $b = 0$, then (5.18) reduces to (5.1) and the physically correct weak solution is given by (5.19) with $d = 0$. If $v_b > u_{we}$, then (5.18) converges to the correct weak solution as $t \to \infty$. This property is used to derive a criterion that excludes the weak solutions described by (ii). In Theorem 5.3 we assume that the solution consists of at most three constant states for all t, in other words, there are no "new" constant states created as time evolves. This assumption is not very restrictive, since in numerical experiments we never observed these "new" constant states. Moreover, we believe that Theorem 5.3 also holds without this assumption, since "new" constant states, not equal to u_u, v_b or u_b, will probably not remain constant as time evolves.

Proof As noted before, the minimum speed for a detonation wave is the speed s_{CJ} of a CJ detonation. It will be useful to consider u_{st} and u_{we} as a function of the wave speed s. Therefore we define two functions $g_{st} : [s_{CJ}, \infty) \to \mathbb{R}$ and $g_{we} : [s_{CJ}, \infty) \to \mathbb{R}$ as (see (4.9) and (4.10))

$$g_{st}(s) := s + \sqrt{(s - u_u)^2 - 2sQ}, \tag{5.21a}$$

$$g_{we}(s) := s - \sqrt{(s - u_u)^2 - 2sQ}. \tag{5.21b}$$

Note that $s_{CJ} = u_{CJ} = g_{st}(s_{CJ}) = g_{we}(s_{CJ})$. From $s - u_u - Q > \sqrt{(s-u_u)^2 - 2sQ}$ it follows that $g'_{we}(s) < 0$ for all $s > s_{CJ}$ and, subsequently, $g_{we}(s) \leq g_{we}(s_{CJ}) = u_{CJ}$. Using this together with $g_{st}(s) \geq s \geq s_{CJ} = u_{CJ}$ we derive

$$u_{we} \leq u_{CJ} \leq u_{st}. \tag{5.22}$$

It is clear that (4.6), (5.17) and $v_b = u_b$ imply $S_2 = s$, i.e. (i) holds and u is given by (5.19) with $d = b$. The remainder of the proof ($v_b \neq u_b$) is given in two steps. In step 1 it is shown that if $v_b > u_b$, then for t sufficiently large the weak solution of (4.1)-(5.18) is given by (5.19) with $d > b$. In step 2 it is shown that for $v_b < u_b$, we must distinguish two cases. If $S_2 < s$, then the weak solution of (4.1)-(5.18) is given by (5.19) with $a < d < b$. On the other hand, if $S_2 \geq s$, then (5.20) describes the weak solution of (4.1)-(5.18) (i.e. (ii) holds).

Step 1. In this step it is assumed that $v_b > u_b$. It follows from this, $u_b \geq s \geq s_{CJ} = u_{CJ}$ and (5.22) that v_b is the final state of a strong detonation and therefore, $v_b > S_2$. Furthermore, $v_b > u_b$ implies that the detonation wave, which connects the state $(u_u, 1)^T$ with $(v_b, 0)^T$, is followed by a rarefaction wave consisting of a smooth transition from $(v_b, 0)^T$ to $(u_b, 0)^T$. However, this solution is unstable, since the head of the rarefaction wave is propagating with a speed $v_b > S_2$. Hence, as t increases the rarefaction wave will overtake the detonation wave and slows it down until the propagation speed is equal to s and the state behind the detonation wave becomes u_b (see left figure in Figure 3). Hence, the weak solution of (4.1)-(5.18) is given by (5.19) with $d > b$ for t sufficiently large.

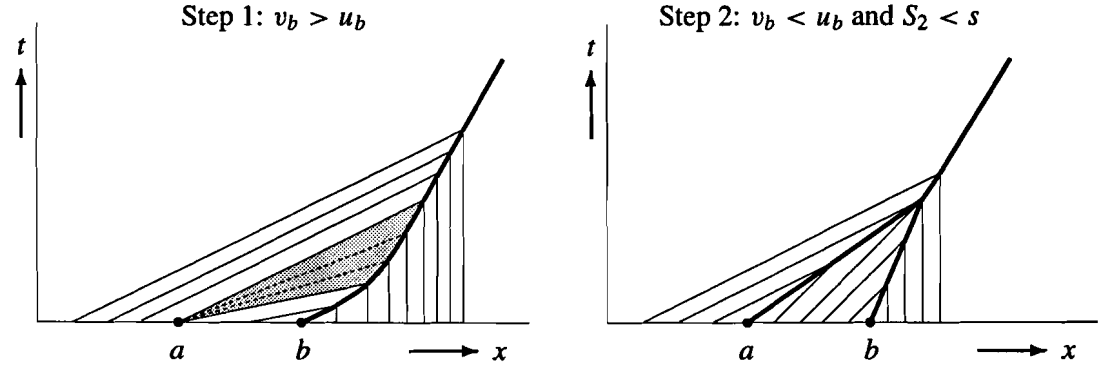

Figure 3: Characteristics corresponding to the formation of the solution (5.19) as described in the proof of Theorem 5.3.

Step 2. Suppose that $v_b < u_b$ and $S_2 < s$. In this case the detonation wave is followed by a shock wave, which connects $(v_b, 0)^T$ with $(u_b, 0)^T$. Let $\bar{S}$ denote the speed of this shock wave, i.e. $\bar{S} = (u_b + v_b)/2$. Using this together with (4.6) and (5.17), we obtain

$$\begin{aligned} \bar{S}(u_b - v_b) &= \tfrac{1}{2}u_b^2 - \tfrac{1}{2}v_b^2 = \tfrac{1}{2}u_b^2 - \tfrac{1}{2}u_u^2 - S_2(v_b - u_u - Q) \\ &= s(u_b - u_u - Q) - S_2(v_b - u_u - Q) \\ &> S_2(u_b - u_u - Q) - S_2(v_b - u_u - Q) = S_2(u_b - v_b). \end{aligned}$$

Hence $\bar{S} > S_2$ and therefore this solution is also unstable, since the shock wave will overtake the detonation wave and accelerates it until the detonation is propagating with speed s and the state behind the detonation wave is equal to u_b (see right figure in Figure 3). Therefore, for t sufficiently large the weak solution of (4.1)-(5.18) is given by (5.19) with $a < d < b$.

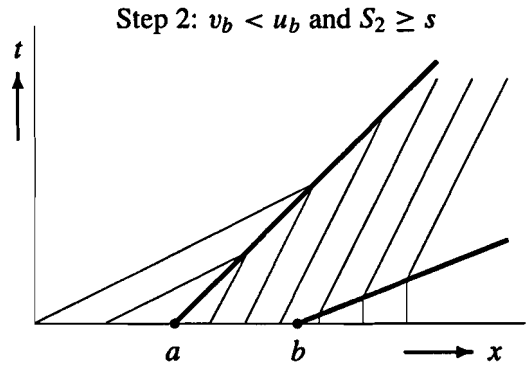

Figure 4: Characteristics corresponding to the solution (5.20) as described in the proof of Theorem 5.3.

Finally we consider the case $v_b < u_b$ and $S_2 \geq s$. Suppose that $v_b \geq S_2$. Using this together with the fact that g_{st} is increasing and $S_2 \geq s$, we deduce $v_b = g_{st}(S_2) \geq g_{st}(s) = u_b$. This is in contradiction with $v_b < u_b$, so $v_b < S_2$ and thus the detonation wave is a weak detonation wave (see Section 4.2). The detonation wave is followed by a shock wave, which connects $(v_b, 0)^T$ to $(u_b, 0)^T$. Again we denote the speed of the shock wave by $\bar{S}$, i.e. $\bar{S} = (u_b + v_b)/2$. Similarly to the previous case ($S_2 \leq s$) we can prove that $\bar{S} \leq S_2$ and the shock will not overtake the detonation wave as time evolves (see Figure 4). This is the stable solution described by (ii). It is clear that in this case the weak solution u is given by (5.20). It follows directly from the fact that g_{we} is decreasing and $S_2 \geq s$ that $v_b = g_{we}(S_2) \leq g_{we}(s) = u_{we}$. This completes the proof. □

Hence, weak detonation waves will not occur or disappear as time evolves, if $v_b > u_{we}$. Remember that due to a shock wave propagating into the unburnt gas, u increases above the ignition temperature and a reaction is started. Therefore, it seems reasonable to assume that no chemical reaction occurs in the cell $[x_{i-1/2}, x_{i+1/2})$ during the $(n+1)$st time step, if $C_i^n < u_{ign}$ (see (4.2), (5.4)). After substituting (5.6a) in (5.6b), using (4.2) and (5.4), we can rewrite (5.6) as

$$U_i^{n+1} = C_i^n + \frac{\Delta t Da}{1 + \Delta t Da} Q H(C_i^n - u_{ign}) Y_i^n, \tag{5.23a}$$

$$Y_i^{n+1} = \frac{1}{1 + \Delta t Da H(C_i^n - u_{ign})} Y_i^n, \tag{5.23b}$$

where H is the Heavyside function defined by $H(x) = 1$ if $x \geq 0$ and $H(x) = 0$ if $x < 0$. Now suppose that in some cell $[x_{i_0-1/2}, x_{i_0+1/2})$ the gas is burnt during the $(n+1)$st time step, i.e. $C_{i_0}^n \geq u_{ign}$ and $Y_{i_0}^n = 1$. Then (5.23a) implies that

$$U_{i_0}^{n+1} \geq u_{ign} + \frac{\Delta t Da}{1 + \Delta t Da} Q. \tag{5.24}$$

Note that $U_{i_0}^{n+1}$ is the state immediately behind the detonation wave and therefore can be interpreted as the quantity v_b^n as defined in (5.9). Using Theorem 5.2 and Theorem 5.3 we should require that $v_b^n > u_{we}$ in order to exclude nonphysical weak detonations. Hence, using $U_{i_0}^{n+1} \approx$

$v_b^n > u_{we}$ and (5.24) it seems useful to require that the following inequality holds

$$u_{ign} + \frac{\Delta t\, Da}{1 + \Delta t\, Da} Q \;>\; u_{we}. \tag{5.25}$$

It is expected that if (5.25) is satisfied, then $v_b^n > u_{we}$ and subsequently $S_2^n \geq s_{CJ}$. In general $\Delta t\, Da$ will be very large and (5.25) reduces to $u_{ign} + Q > u_{we}$. It seems that the nonphysical weak detonation waves are only observed if u_{ign} is close to u_u. Since $u_u + Q < u_{we}$ (see (4.6) and $s > 0$), inequality (5.25) is not satisfied and due to numerical diffusion, u is raised above the ignition temperature and an artificial reaction is started. If Da is large enough, then the gas is completely burnt in the next time step Δt and the discontinuity is shifted to a cell boundary. Therefore, it is not surprising that nonphysical wave speeds of one cell per time step can be observed for large Da [3, 8].

However, numerical experiments in the next section illustrate that for physically more realistic values of u_{ign}, (5.25) is satisfied and, subsequently, $v_b = u_b$.

6 Numerical Results for the Simplified Detonation Model

In this section numerical results are presented for the method (5.23). In the first example it is shown that for small mesh sizes, the numerical solution is a physically correct strong detonation wave. However, if the mesh width is increased to more practical values, then the solution becomes a nonphysical weak detonation wave. In all the examples the sequence S_2^n converges. The further examples clearly illustrate that criterion (5.25) is a useful criterion to exclude nonphysical solutions.

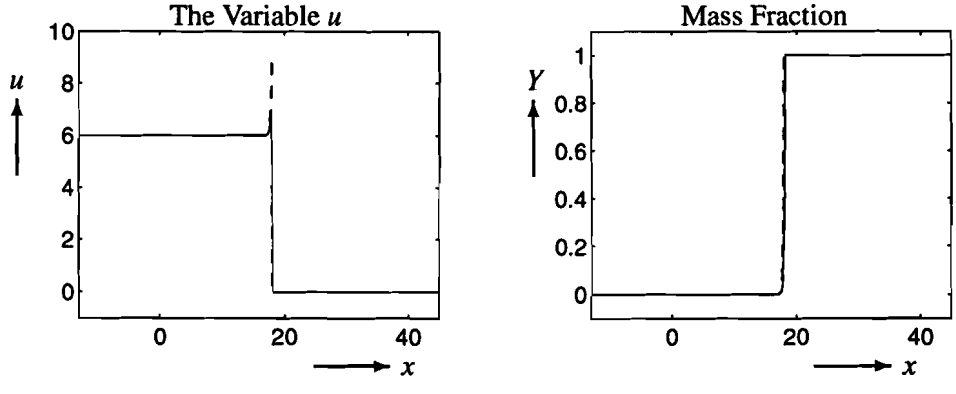

Figure 5: Exact solution (dashed line) and numerical solution (solid line) at $t = 4$ of a strong detonation with $Q = 2$, $f = 1.265625$, $Da = 31.192$ (1 pt/$L_{1/2}$), $u_{ign} = 0.1$, $\Delta t = 0.01$ and $\Delta x = 0.1$.

Example 6.1 In this example we consider the same strong detonation as in Example 4.1. If the method (5.23) is used with initial data (5.1), then after some period a ZND profile is formed. The numerical solution is then propagating with a constant numerical wave speed S. However, in this example we want to study the behaviour of the numerical detonation wave as time evolves and not the formation of a ZND profile. Therefore, we use initial data corresponding to the exact ZND solution of the strong detonation (see Figure 2). Moreover, with these initial data we can compute the exact solution of (4.1) easily, namely $\mathrm{u}(x, t) = \mathrm{u}^0(x - st)$, where $s = 4.5$ is the

exact wave speed of the detonation wave. This implies that we are able to compare the numerical results with the exact solution.

In Figure 5 the numerical results are compared with the exact solution. The mesh width $\Delta x = 0.1$ and the time step $\Delta t = 0.01$. The numerical ZND profile is essentially correct and the numerical wave speed is equal to the exact wave speed. However, the mesh width is relatively small and in most practical cases we cannot afford such fine meshes.

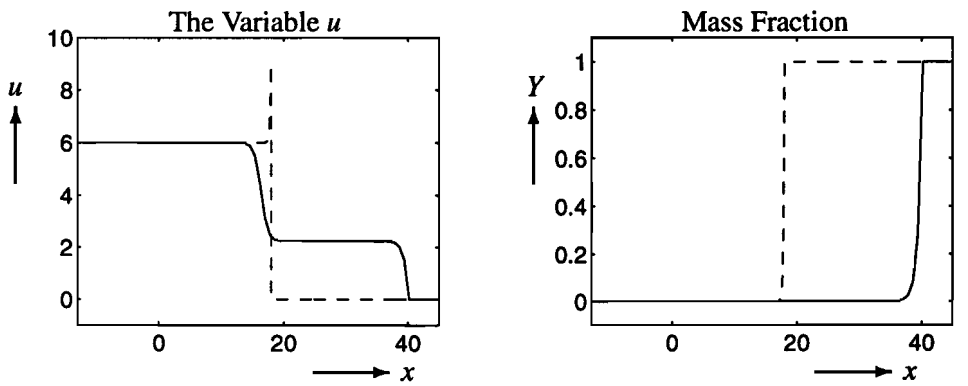

Figure 6: Exact solution (dashed line) and numerical solution (solid line) at $t = 4$ of a strong detonation with $Q = 2$, $f = 1.265625$, $Da = 31.192$ (0.125 pts/$L_{1/2}$), $u_{ign} = 0.1$, $\Delta t = 0.08$ and $\Delta x = 0.8$.

Therefore, we increase Δx and Δt and keep $\tau = \Delta t/\Delta x$ fixed. The exact ZND solution should still propagate with a wave speed $s = 4.5$. However, Figure 6 clearly illustrates that the numerical solution is completely wrong. As predicted by Theorem 5.2, there is a weak detonation wave propagating with a numerical wave speed $S_2 > s$. In this weak detonation wave all heat is released and the gas is completely burnt. In this case $S_2 = 10$ and $v_b = 2.2540 < u_{we} = 3$ (note that (5.17) is satisfied). Inequality (5.25) is not satisfied since $u_{ign} + \Delta t Da Q/(1 + \Delta t Da) = 1.5278 < u_{we}$.

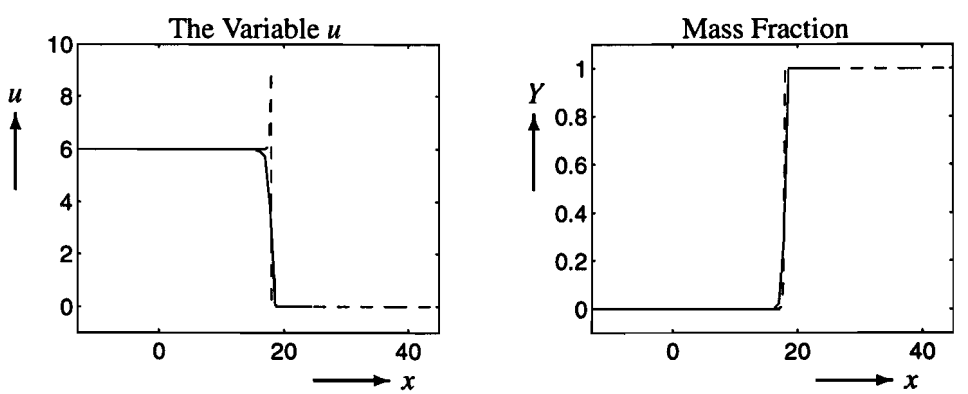

Figure 7: Exact solution (dashed line) and numerical solution (solid line) at $t = 4$ of a strong detonation with $Q = 2$, $f = 1.265625$, $Da = 31.192$ (0.125 pts/$L_{1/2}$), $u_{ign} = 1.6$, $\Delta t = 0.08$ and $\Delta x = 0.8$.

Next the numerical solution is computed with $u_{ign} = 1.6$. In this case (5.25) is fulfilled, since $u_{ign} + \Delta t Da Q/(1 + \Delta t Da) = 3.0278 > u_{we}$. In Figure 7 the solution is drawn. The numerical detonation wave solution is the correct strong detonation wave. The peak in the variable

u is completely disappeared. This is caused by the combination of a large mesh size and a thin reaction zone. The reaction is so fast that even in the initial data $\mathrm{U}_i^0 = \bar{\mathrm{u}}_i^0$ no peak is noticeable. Comparing the results in Figure 7 to the results in Figure 6, the improvement is convincing.

In Figures 5 and 6 the ignition temperature u_{ign} is close to u_u. However, in practice the ignition temperature is much higher than u_u. Therefore, we expect that in most realistic cases (5.25) is satisfied. In the following example it is illustrated that (5.25) is a useful criterion. We restrict ourselves to very fast reactions (or large mesh sizes), since in these cases the wrong solutions occur.

Example 6.2 In this example we consider again the strong detonation described in Example 4.1. In order to investigate the practical use of (5.25), we choose initial data corresponding to a nonphysical solution as described by Theorem 5.2. Subsequently, we examine whether this solution has a temporally constant profile or transforms into the physically correct detonation wave as time evolves. Let the initial data be given by (see (5.18))

$$(u^0(x), Y^0(x))^T = \begin{cases} (u_{st}, 0)^T, & x < -30, \\ (u_{we}, 0)^T, & -30 < x < 0, \\ (u_u, 1)^T, & x > 0, \end{cases} \tag{6.1}$$

where $u_{st} = 6$, $u_{we} = 3$ and $u_u = 0$. Analogously to Theorem 5.3, v_b denotes the value of u behind the numerical detonation wave, so initially $v_b = u_{we}$. Furthermore, $\Delta t = 0.125$, $Da = 3.1192 \cdot 10^5$ and $Q = 2$, so (5.25) is rewritten as $u_{ign} + 2 > u_{we} = 3$. It is straightforward that $L_{1/2} = 10^{-5}$.

The results in Table 8 clearly show that if (5.25) is satisfied, the weak detonation wave is unstable and after some period (5.23) will approximate the correct strong detonation wave.

u_{ign}	S_2	v_b	(5.25) satisfied
0.2	9.000	2.2917	no
0.4	5.580	2.6017	no
0.8	4.500	3.0000	no
1.0	4.500	3.0000	no
1.1	4.500	6.0000	yes
1.2	4.500	6.0000	yes

Table 8: Numerical results with $Q = 2$, $f = 1.265625$, $Da = 3.1192 \cdot 10^5$ $((8/9) \cdot 10^{-5}$ pts/$L_{1/2})$, $\Delta x = 1.125$, $\Delta t = 0.125$ and initial data (6.1).

7 Numerical Results for the Reactive Euler Equations

In this section we consider the reactive Euler equations (3.1), as described in Section 3. We assume that the initial data correspond to the exact ZND solution of a CJ or strong detonation.

Analogously to Section 5, we solve (3.1) with a first order splitting method. The first step of the method consists of Roe's first order method for gas dynamics with an extra advected quantity Y. Let $\tilde{g}_i^n$ denote the result in the ith cell after the first step, for all variables g. In the second step

the backward Euler method is used to solve the corresponding ordinary differential equation. The final solution at time t^{n+1} is given by

$$\rho_i^{n+1} = \tilde{\rho}_i^n, \qquad u_i^{n+1} = \tilde{u}_i^n,$$
$$E_i^{n+1} = \tilde{E}_i^n, \qquad Y_i^{n+1} = \begin{cases} \tilde{Y}_i^n, & \tilde{T}_i^n < T_{ign}, \\ \dfrac{1}{1+\Delta t Da}\tilde{Y}_i^n, & \tilde{T}_i^n \geq T_{ign}. \end{cases} \tag{7.1}$$

Analogously, to (5.7b) we define a quantity S^n at time t^n as

$$-S^n n\Delta t = \Delta x \sum_{i=-\infty}^{\infty} \left(Y_i^n - Y_i^0\right), \tag{7.2}$$

where Y is the mass fraction of the unburnt gas. Again, S^n can be interpreted as the average speed of the numerical detonation wave at time level t^n.

Now suppose that in the cell $[x_{i_0-1/2}, x_{i_0+1/2})$ the gas is burnt during the $(n+1)$st time step, i.e. $\tilde{T}_{i_0}^n \geq T_{ign}$ and $\tilde{Y}_{i_0}^n > 0$. Contrary to (5.24), for the reactive Euler equations $\tilde{Y}_{i_0}^n \neq 1$ in general. In the first step of the splitting method Y is simply advected along the contact discontinuity and therefore in some "unburnt cells" Y will decrease beneath 1. Hence, we only know that $0 \leq \tilde{Y}_{i_0}^n \leq 1$. It follows from (3.2) and (3.4) that

$$\tilde{T}_{i_0}^n = (\gamma-1)(\tilde{E}_{i_0}^n - \tfrac{1}{2}(\tilde{u}_{i_0}^n)^2 - Q\tilde{Y}_{i_0}^n).$$

Using this together with (7.1), it is easy to see that (see (5.24))

$$\begin{aligned} T_{i_0}^{n+1} &= \tilde{T}_{i_0}^n + (\gamma-1)\,Q\,(\tilde{Y}_{i_0}^n - Y_{i_0}^{n+1}) \\ &\geq T_{ign} + \frac{\Delta t Da}{1+\Delta t Da}(\gamma-1)\,Q\,\tilde{Y}_{i_0}^n. \end{aligned}$$

Analogously to (5.25) we require that the following inequality holds

$$T_{ign} + \frac{\Delta t Da}{1+\Delta t Da}(\gamma-1)\,Q\,\tilde{Y}_{i_0}^n > T_{we}, \tag{7.3}$$

where T_{we} is the final temperature of the corresponding weak detonation wave propagating with speed s. The quantity T_{we} is given by a complicated algebraic expression, see [11]. In general $\Delta t Da$ will be very large and (7.3) reduces to $T_{ign} + (\gamma-1)Q\tilde{Y}_{i_0}^n > T_{we}$.

As noted before, for fast reactions it is possible to obtain stable numerical solutions of the reactive Euler equations that look reasonable and yet are completely wrong, because the discontinuities have the wrong locations. Thus, the numerical reaction waves are propagating at nonphysical wave speeds [3]. These "wrong solutions" turn out to be nonphysical weak detonation waves. Analogously to the simplified detonation model, the nonphysical weak detonation waves are only observed when the ignition temperature is close to the temperature of the unburnt gas. However, in practical applications the ignition temperature is much higher. Hence, for higher ignition temperatures we expect that (7.3) will be satisfied and, subsequently, that the nonphysical weak detonations will not occur. We now present some numerical results that support this statement.

In all examples we consider the ZND solution of the strong detonation described in Example 3.1. However, we increase the Damköhler number to $Da = 0.6.7486 \cdot 10^5$, since for fast reactions the nonphysical weak detonations occur. The half reaction length $L_{1/2}$ becomes $L_{1/2} = 10^{-6}$.

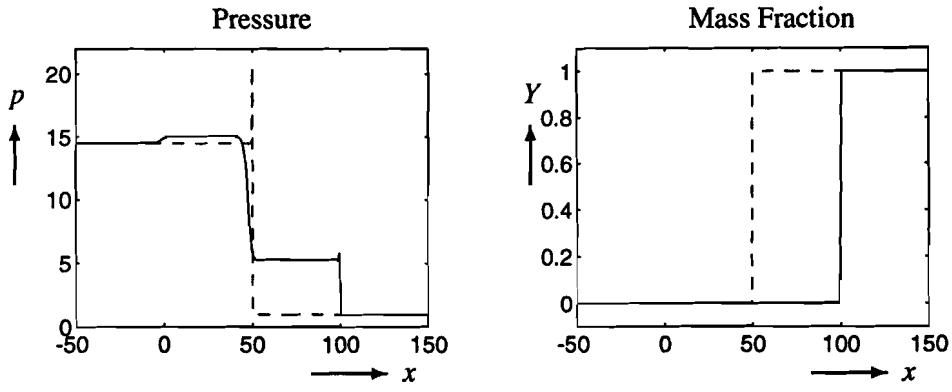

Figure 9: Exact solution (dashed line) and numerical solution (solid line) at $t = 10$ of a stong detonation with $Q = 10$, $\gamma = 1.4$, $T_{ign} = 1.01$, $Da = 6.7486 \cdot 10^5$ (10^{-6} pts/$L_{1/2}$), $\Delta t = 0.1$ and $\Delta x = 1$.

Example 7.1 In this first example we choose a low ignition temperature, namely: $T_{ign} = 1.01$ (note that $T_u = 1$). The results in Figure 9 clearly illustrates that the numerical solution is completely wrong. Analogously to the results of Figure 6, there is a weak detonation wave propagating with a numerical wave speed $S^n = 10 > s = 5$. In this weak detonation wave all energy is released and the gas is completely burnt. With the parameters from Figure 9, (7.3) becomes $T_{ign} + 4\tilde{Y}_{i_0}^n > T_{we}$. However, since $T_{ign} = 1.01$ and $\tilde{Y}_{i_0}^n \leq 1$, we have $T_{ign} + 4\tilde{Y}_{i_0}^n \leq 5.01 < T_{we} = 5.4042$. So, (7.3) is not fulfilled as we expected.

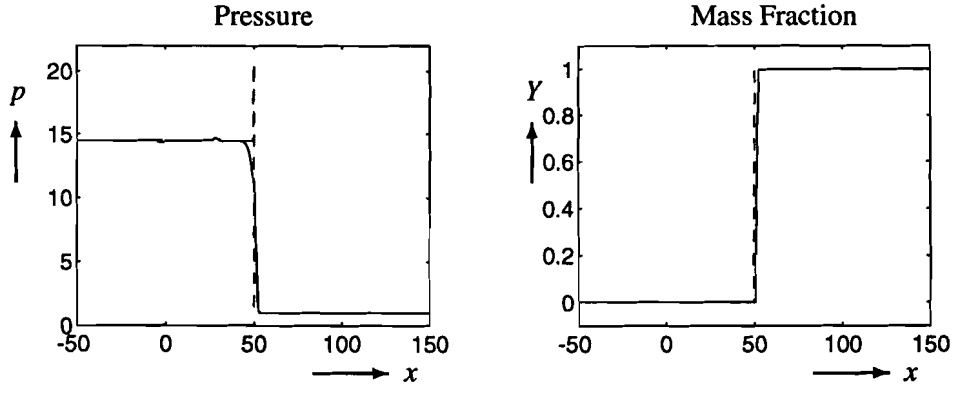

Figure 10: Exact solution (dashed line) and numerical solution (solid line) at $t = 10$ of a stong detonation with $Q = 10$, $\gamma = 1.4$, $T_{ign} = 3.0$, $Da = 6.7486 \cdot 10^5$ (10^{-6} pts/$L_{1/2}$), $\Delta t = 0.1$ and $\Delta x = 1$.

Example 7.2 In this example we choose the ignition temperature significantly larger that T_u, namely $T_{ign} = 3.0$. In Figure 10 the numerical results are compared to the exact solution. Although there is some noise in the pressure behind the shock wave, we see a large improvement of the results compared to Figure 9 (where $T_{ign} = 1.01$). The disturbances behind the shock wave are caused by the splitting method. These oscillations will occur for all Godunov-type methods in combination with a splitting method. Now, (7.3) becomes $3 + 4\tilde{Y}_{i_0}^n > T_{we} = 5.4042$, which is satisfied as $\tilde{Y}_{i_0}^n > 0.60105$. As noted before, in the first step of the splitting method in some

"unburnt cells" Y will decrease beneath 1. However, long before Y reaches 0.60105, the temperature increases above T_{ign} and the gas is burnt. So, (7.3) is satisfied in general, as is clearly illustrated by the numerical results in Figure 10.

Next we consider the numerical wave speed for increasing T_{ign} and study whether (7.3) is satisfied or not. Note that in this case the von Neumann temperature is given by $T_{vN} = 4.4089$ (see Example 3.1), so $1 < T_{ign} < 4.4089$.

In Table 11 the results are shown with $T_{ign} = 1, 2, 3, 4$. If $T_{ign} \geq 3$, then the numerical wave speed S^n approximates the exact wave speed $s = 5$ very well. If $T_{ign} \leq 1.4042$, then (7.3) cannot be satisfied and a weak detonation is formed. In all our examples we observe a switch on phenomenon in which a "numerical detonation wave" is formed. In this initial period the numerical wave speed is a poor approximation of the exact wave speed. Due to our definition of S^n, for reasonable n this is still noticeable in the results in Table 11. In order to overcome this problem we define a quantity $S^{n,m}$ at time t^n for all $n > m$ as (see (7.2)

$$-S^{n,m}(n-m)\Delta t = \Delta x \sum_{i=-\infty}^{\infty} \left(Y_i^n - Y_i^m\right). \tag{7.4}$$

Hence, we assume that after m time steps the switch on phenomenon is finished and $S^{n,m}$ measures the numerical wave speed after the first m time steps. The results in Table 11 show that $S^{n,m}$ is a accurate approximation of the exact wave speed as $T_{ign} \geq 3$. Other authors have used a shock tracking method to enforce the correct wave speed [2]. Numerical computations show that these shock tracking methods produce similar wave speeds as the results in Table 11.

T_{ign}	S^n	$S^{n,m}$	$\lvert\frac{S^{n,m}-s}{s}\rvert$
1.0	10.000	10.000	$0.1000 \cdot 10^{+1}$
2.0	5.1001	5.0572	$0.1144 \cdot 10^{-1}$
3.0	5.0125	5.0000	$0.3053 \cdot 10^{-7}$
4.0	5.0010	5.0000	$0.1417 \cdot 10^{-7}$

Table 11: Numerical results at $t = 100$ with $Q = 10$, $\gamma = 1.4$, $Da = 6.7486 \cdot 10^5$ (10^{-6} pts/$L_{1/2}$), $n = 1000$, $m = 500$, $\Delta t = 0.1$ and $\Delta x = 1$.

References

[1] A.C. Berkenbosch, E.F. Kaasschieter and J.H.M. ten Thije Boonkkamp, *Finite-difference methods for one-dimensional hyperbolic conservation laws*, Num. Meth. for Part. Diff. Eq. **10** (1994), pp. 225-269.

[2] A. Bourlioux, A. Majda and V. Roytburd, *Theoretical and numerical structure for unstable one-dimensional detonations*, SIAM J. Appl. Math. **51** (1991), pp. 303-343.

[3] P. Colella, A. Majda and V. Roytburd, *Theoretical and numerical structure for reacting shock waves*, SIAM J. Sci. Stat. Comput. **7** (1986), pp. 1059-1080.

[4] R. Courant and K.O. Friedrichs, Supersonic Flow and Shock Waves, Wiley, New York (1948).

[5] W. Fickett and W.C. Davis, Detonation, University of California Press, Berkeley (1979).

[6] J. Goettgens, F. Mauss and N. Peters, Analytic Approximations of Burning Velocities and Flame Thicknesses of Lean Hydrogen, Methane, Ethylene, Acethylene and Propane Flames, 24th Intl. Symp. on Combustion, The Combustion Institute, Pittsburgh (1992).

[7] P.D. Lax, Hyperbolic Systems of Conservation Laws and the Mathematical Theory of Shock Waves, SIAM Regional Conference Series in Applied Mathematics, volume 11, SIAM, Philadelphia (1973).

[8] R.J. LeVeque and H.C. Yee, *A study of numerical methods for hyperbolic conservation laws with stiff source terms*, J. Comput. Phys. **86** (1990), pp. 187-210.

[9] A. Majda, *A qualitative model for dynamic combustion*, SIAM J. Appl. Math. **41** (1981), pp. 70-93.

[10] R.A. Strehlow, Combustion Fundamentals, McGraw-Hill, New York (1984).

[11] F.A. Williams, Combustion Theory, The Fundamental Theory of Chemically Reacting Flow Systems, Addison-Wesley, Redwood City (1985).